Inorg. Chem. **2005**, *44*, 3249–3260

Coordination Behavior toward Copper(II) and Zinc(II) Ions of Three Ligands Joining 3-Hydroxy-2-pyridinone and Polyaza Fragments

Gianluca Ambrosi,[†] Mauro Formica,[†] Vieri Fusi,*[,†] Luca Giorgi,[†] Annalisa Guerri,[‡] Simone Lucarini,[§] Mauro Micheloni,*[,†] Paola Paoli,[‡] Patrizia Rossi,[‡] and Giovanni Zappia[§]

Institute of Chemical Sciences and Institute of Pharmaceutical Chemistry, University of Urbino, P.za Rinascimento 6, I-61029 Urbino, Italy, and Department of Energy Engineering "Sergio Stecco", University of Florence, Via S. Marta 3, I-50139 Florence, Italy

Received November 3, 2004

The synthesis and characterization of new polydentate ligand 2-(*N*),2′-(*N*′)-bis[2-(3-hydroxy-2-oxo-2*H*-pyridin-1-yl)-acetamido]-1(*N*′),2(*N*),2′(*N*′)-trimethyl-2,2′-diaminodiethylamine (**L3**) is reported. The coordination properties of **L3** and of two analogous macrocyclic ligands (**L1** and **L2**) toward Cu(II) and Zn(II) metal ions are reported. All three ligands show the 3-hydroxy-2(1*H*)-pyridinone (HPO) groups attached as sidearms to a polyaza fragment, which is a macrocyclic framework in the case of **L1** and **L2** while it is an open chain in the case of **L3**. The role of the polyaza fragments in preorganizing the two sidearms was investigated. The basicity of **L3** and the binding properties of **L1**–**L3** were determined by means of potentiometric measurements in aqueous solution (298.1 ± 0.1 K, I = 0.15 mol dm^{-3}). UV–vis spectra as well ^{1}H and ^{13}C NMR experiments were used to understand the role of the HPO and of the polyaza fragments in the stabilization of the cations. While **L1** forms stable mono- and dinuclear complexes, **L2** and **L3** can form only mononuclear species with each of the metal ions investigated. In the main mononuclear species of **L2** and **L3**, the two HPO moieties stabilize the M(II) in a square planar geometry due to the two oxygen atoms of each HPO. The coordination sphere of the metal is completed by adding a secondary ligand such as water molecules in the case of Cu(II) systems or OH$^-$ in the Zn(II) systems. These results are confirmed by the crystal structures of the [CuH$_{-1}$**L2**]$^+$ and [CuH$_{-1}$**L3**]$^+$ species reported herein. Two conformations of **L1** can be hypothesized in the formation of the dinuclear species, as suggested by NMR experiments on the [ZnH$_{-2}$**L1**] species, which shows two conformers slowly interchanging on the NMR time scale, one of which was found to be more insoluble.

Introduction

The coordination of transition metal ions has continued to attract interest and development ever since the origin of modern coordination chemistry. The aim of understanding the thermodynamic parameters and their role in the formation of the complexes has been a driving force for many years.[1,2] In the last 20 years, great attention has been addressed to the design and synthesis of ligands able to bind specific metals and to obtaining specific conformations of the complex formed.[3−5] In this field, some of the main drivers of research can be found in the development of chemical sensors and new materials;[6−8] however, new impulses have

* Authors to whom correspondence should be addressed. E-mail: vieri@chim.uniurb.it (V.F.).
[†] Institute of Chemical Sciences, University of Urbino.
[‡] Department of Energy Engineering "Sergio Stecco", University of Florence.
[§] Institute of Pharmaceutical Chemistry, University of Urbino.

(1) (a) Pedersen, C. J. *J. Am. Chem. Soc.* **1967**, *89*, 7017. (b) Lehn, J. M. *Pure Appl. Chem.* **1977**, *49*, 857. (c) Cram, D. J.; Cram, J. M. *Science* **1984**, *183*, 4127. (d) Lehn, J. M. *Angew. Chem., Int. Ed. Engl.* **1988**, *27*, 89.
(2) (a) Martell, A. E.; Motekaitis, R. J. *Determination and Use of Stability Constants*, 2nd ed.; Wiley-VCH: New York, 1992. (b) Connors, K. A. *Binding Constant, The Measurement of Molecular Complex Stability*; Wiley-Interscience: New York, 1987.
(3) (a) Zelewsky, A. *Stereochemistry of Coordination Compounds*; John Wiley & Sons: New York, 1996. (b) Martell, A. E.; Constable, E. C. *Coordination Chemistry of Macrocyclic Compounds*; Oxford University Press: New York, 1999. (b) Bianchi, A.; Micheloni, M.; Paoletti, P. *Coord. Chem. Rev.* **1991**, *110*, 17.
(4) Hancock, R. D. Metal Complexes in Aqueous Solution. *Modern Inorganic Chemistry*; Plenum Press: New York, 1996.
(5) Formica, M.; Fusi, V.; Micheloni, M.; Pontellini, R.; Romani, P. *Coord. Chem. Rev.* **1999**, *184*, 347.
(6) Gokel, G. W.; Leevy, W. M.; Weber, M. E. *Chem. Rev.* **2004**, *104*, 2723.
(7) Zolotov, Y. A. *Macrocyclic Compounds in Analytical Chemistry*; Wiley- Interscience: New York, 1997.

10.1021/ic0484607 CCC: $30.25
Published on Web 03/30/2005

been given by the better understanding we now have of the processes, reactivity, and structure of biological functions.[9−12] Indeed, many of these are based on transition metal centers, which in many cases cooperate with each other, thus inspiring chemists to produce synthetic metal receptors mimicking the active site and/or reproducing the biological activity. Seen in this light, many of the biological active centers are formed by a mono- or bimetallic core and make the design of new ligands able to form stable mono- and dinuclear complexes prone to interaction with further substrates interesting. The comparison between mono- and bimetallic complexes is also attractive; in fact, it should also be considered that bimetallic systems can provide new reactivity patterns and physical properties that could not be achieved by similar mononuclear complexes. In this sense, many metal cations could be considered, but Cu(II) and Zn(II) ions are undoubtedly two of the most interesting metals in that they often constitute the mono- or dinuclear core of the active site of the biological functions and their complexes can be used in many applications; for example, their complexes have been recently used as sensors of an external species such phosphate and others.[13−15]

Recently, we reported the synthesis of two new ligands showing two 3-hydroxy-2(1*H*)-pyridinone (HPO) groups attached as sidearms to the macrocyclic base 1,7-dimethyl-1,4,7,10-tetrazacyclododecane, Me_2[12]aneN_4 (**L1** and **L2** in Figure 1).[16,17] The reason was to exploit the coordination properties of the HPO as sidearm groups by preorganizing its coordination of the metal cations. Molecular modeling and crystal structures of both ligands highlighted that the way in which the two HPO groups are connected to the macrocyclic Me_2[12]aneN_4 base is fundamental to stiffen and preorganize the host. In fact, the N−C═O amide group of **L2**, which links each HPO moiety to the 12-membered ring,

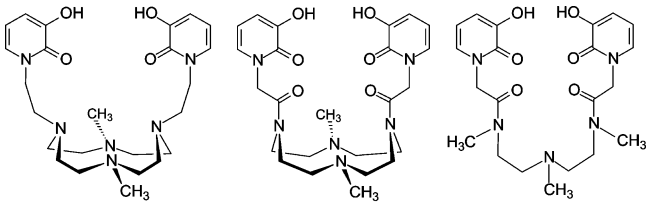

Figure 1. Schematical drawing of ligands **L1**−**L3**.

draws the two sidearms to occupy the same region with respect to the macrocycle base more efficiently compared to the N−CH_2 group of **L1**. This aspect implies that **L2** is a more efficient ligand than **L1** in binding in aqueous solution substrates such as ammonium and alkali and alkaline earth cations, for which the interaction is mainly based on electrostatic forces. In these cases, only the formation of L/guest adducts having 1:1 molar ratio was observed. Nevertheless, when the HPO groups are linked by means of an amine N−CH_2 function as in **L1**, the macrocyclic base furnishes a further tetraamine coordination area which is not available in the case of **L2**. This area should be suitable to bind transition metal ions such as Cu(II) and Zn(II); thus, **L1**, on the contrary to **L2**, it is also able to stabilize two metal ions by forming dinuclear species in which the two M(II) centers are probably displaced close to each other.

In this paper, we report the synthesis of the new ligand **L3** (Figure 1) which was synthesized to investigate the influence that the macrocyclic base plays in preorganizing the HPO to stabilize Cu(II) and Zn(II) cations. In fact, **L3** again shows two HPO groups linked, in the same way as **L2**, to a linear fragment resembling the triaza chain of **L2**.

The binding properties toward Cu(II) and Zn(II) in aqueous solution of the three mentioned ligands are considered and are reported together with the synthesis and the acid−base properties of the new ligand **L3**. Two crystal structures of Cu(II) complexes are also reported.

Experimental Section

General Methods. IR spectra were recorded with a Shimadzu FTIR-8300 spectrometer. Melting points were determined with a Büchi melting point B 540 apparatus and are uncorrected. EI-MS spectra (70 eV) were recorded with a Fisons Trio 1000 spectrometer; ESI mass spectra were recorded with a ThermoQuest LCQ Duo LC/MS/MS spectrometer. UV absorption spectra were recorded at 298 K with a Varian Cary-100 spectrophotometer equipped with a temperature control unit.

Synthesis. Ligand **L3** was obtained by following the synthetic procedure reported in Scheme 1. 3-(Benzyloxy)-1-(carboxymethyl)-2-(1*H*)-pyridinone (**1**)[17,18] and *N*,*N*′-dimethyl-*N*-(2-(methylamino)-ethyl)ethane-1,2-diamine (**3**)[19] were prepared as previously described. All other chemicals were purchased in the highest quality commercially available. The solvents were RP grade, unless otherwise indicated.

(8) Balzani, V.; Credi, A.; Venturi, M. *Molecular Devices and Machines: A Journey into the Nanoworld*; VCH Verlagsgesellschaft Mbh: Weinheim, Germany, 2003.
(9) (a) Lippard, S. J.; Berg, J. M. *Principles of Bioinorganic Chemistry*; University Science Books: Mill Valley, CA, 1994. (b) *Bioinorganic Catalysis*; Reedijk, J., Ed.; Dekker: New York, 1993.
(10) (a) Karlin, K. D. *Science* **1993**, *261*, 701. (b) Wilcox, D. E. *Chem. Rev.* **1996**, *96*, 2435. (c) Hughes, M. N. *The Inorganic Chemistry of the Biological Processes*; Wiley: New York, 1981.
(11) (d) Da Silva, F. J. J. R.; Williams, R. J. P. *The Biological Chemistry of the Elements: The Inorganic Chemistry of Life*; Oxford University Press: New York, 2001.
(12) Gubernator, K.; Böhm, H.-J. *Structure-Based Ligand Design. Method and Principles in Medicinal Chemistry*; Wiley-VCH: Weinheim, Germany, 1998; Vol. 6.
(13) (a) Agnus, Y. L. *Copper Coordination Chemistry: Biochemical and Inorganic Perspective*: Adenine Press: Guilderland, NY, 1983. (b) Bertini, I., Luchinat, C., Marek, W., Zeppezauer, M., Eds. *Zinc Enzymes*; Birkauser: Boston, MA, 1986.
(14) (a) Martell, A. E.; Sawyer, D. T. *Oxygen Complexes and Oxygen Activation by Transition Metals*; Plenum Press: New York, 1987. (b) Schindler, S. *Eur. J. Inorg. Chem.* **2000**, 2311. (c) Davies, M. B. *Coord. Chem. Rev.* **1996**, 1. (c) Aoki, S.; Kimura, E. *J. Am. Chem. Soc.* **2000**, *122*, 4542.
(15) Meunier, B. *Biomimetic Oxidations Catalyzed by Transition Metal Complexes*; Imperial College Press: London, 2000.
(16) Formica, M.; Fusi, V.; Giorgi, L.; Guerri, A.; Lucarini, S.; Micheloni, M.; Paoli, P.; Pontellini, R.; Rossi, P.; Tarzia, G.; Zappia, G. *New J. Chem.* **2003**, *27*, 1575
(17) Ambrosi, G.; Dapporto, P.; Formica, M.; Fusi, V.; Giorgi, L.; Guerri, A.; Lucarini, S.; Micheloni, M.; Paoli, P.; Pontellini, R.; Rossi, P.; Zappia, G. *New J. Chem.* **2004**, *28*, 1359.
(18) Streater, M.; Taylor, P. D.; Heider, R. C.; Porter, J. *J. Med. Chem.* **1990**, *33*, 1749.
(19) Bencini, A.; Bianchi, A.; Garcia-España, E.; Fusi, V.; Micheloni, M.; Paoletti, P.; Ramirez, J. A.; Rodriguez, A.; Valtancoli, B. *J. Chem. Soc., Perkin Trans. 2* **1992**, 1059−1065.

Scheme 1. Synthesis of Ligand **L3**

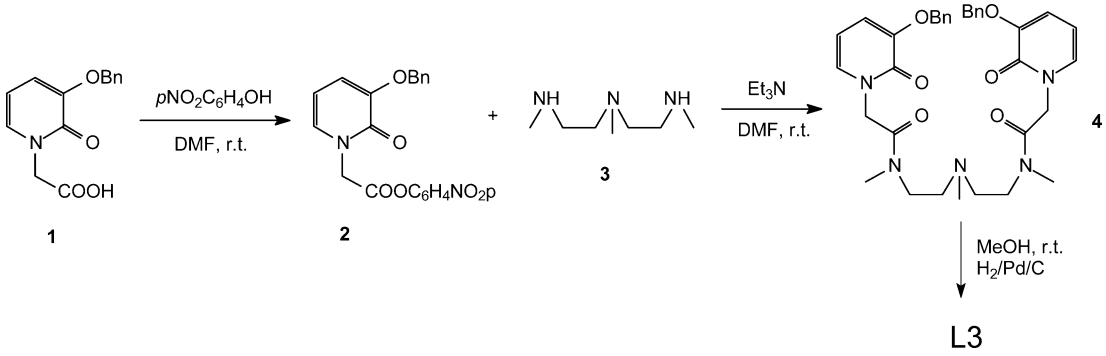

4-Nitrophenyl 2-(3-(Benzyloxy)-2-oxopyridin-1(2*H*)-yl)acetate (2). To a well stirred solution of 3-(benzyloxy)-1-(carboxymethyl)-2-(1*H*)-pyridinone (**1**) (2 g, 7.72 mmol) in dry DMF (2 mL) at 0 °C were added a solution of 4-nitrophenol (1.13 g, 8.11 mmol) in dry DMF (2 mL) and a solution of 1,3-dicyclohexylcarbodiimide (1.67 g, 8.11 mmol) in dry DMF (2 mL) dropwise under N_2. The reaction was stirred at room temperature in the dark overnight whereupon acetic acid (0.2 mL) was added and the mixture stirred for an additional 1 h. After that time the mixture was filtered over Celite and concentrated under reduced pressure. The brown solid residue was purified by crystallization (ethyl acetate) to afford **2** (2.35 g, 80%) as yellow-brown needles: mp 121−123 °C dec; MS *m*/*z* (EI) 380 $[M]^+$, 242 $[M - OPhNO_2]^+$, 289 $[M - CH_2Ph]^+$; ^{1}HNMR ($CDCl_3$) δ 8.30−8.24 (m, 2H), 7.42−7.30 (m, 7H), 6.95 (dd, J = 1.6 Hz, J = 6.8 Hz, 1H), 6.72 (dd, J = 1.7 Hz, J = 7.5 Hz, 1H), 6.14 (t, J = 7.1 Hz, 1H), 5.14 (s, 2H), 4.88 (s, 2H); ^{13}C NMR ($CDCl_3$) δ 165.47, 154.94, 148.98, 140.83, 135.92, 128.93, 128.14, 127.36, 125.27, 122.40, 116.10, 105.53, 70.88, 51.33.

***N*,*N*′-Dimethyl-*N*,*N*′-bis[2-(3-(benzyloxy)-2-oxo-2*H*-pyridin-1-yl)acetamido]-*N*-(2-(methylamino)ethyl)ethane-1,2-diamine (4).** A solution of 4-nitrophenyl 2-[3-(benzyloxy)-2-oxopyridin-1(2*H*)-yl]acetate (2) (1.38 g, 3.63 mmol) in dry DMF (3 mL) was added dropwise at 0 °C to a stirred solution of *N*,*N*′-dimethyl-*N*-(2-(methylamino)ethyl)ethane-1,2-diamine (3) (0.26 g, 1.82 mmol) and Et_3N (1.01 mL, 7.26 mmol) in dry DMF (3 mL) under nitrogen. The reaction was stirred for 2 h at room temperature and then concentrated under vacuum before the addition of ethyl acetate (200 mL). The solution was washed with 5% aqueous $NaHCO_3$ (3 × 100 mL) and brine (2 × 50 mL), dried over Na_2SO_4, and concentrated under vacuum. The residue was purified by silica gel chromatography (98:2 CH_2Cl_2/MeOH) to give the protected ligand **4** (0.74 g, 65%) as a white solid: mp 102−104 °C dec; IR (film) 2959, 1654, 1605, 1252 cm^{-1}; MS *m*/*z* (ESI) 650.3 ($[M + Na]^+$), 628.3 ($[M + 1]^+$); ^{1}HNMR ($CDCl_3$) δ 7.39−7.27 (m, 10H), 7.01−6.92 (m, 2H), 6.66−6.59 (m, 2H), 6.05−5.93 (m, 2H), 5.28 (s, 4H), 4.80−4.73 (m, 4H), 3.59−3.42 (m, 4H), 3.13−2.94 (m, 6H), 2.79−2.56 (m, 4H), 2.40−2.29 (m, 3H); ^{13}CNMR ($CDCl_3$) δ 167.07, 166.86, 158.16, 148.54, 136.34, 130.59, 130.36, 128.55, 127.96, 127.35, 116.02, 115.68, 104.49, 104.36, 70.76, 56.28, 55.31, 55.16, 54.52, 49.63, 49.40, 49.25, 48.53, 45.87, 43.01, 35.32, 35.12, 34.45.

2-(*N*),2′-(*N*′)-Bis[2-(3-hydroxy-2-oxo-2*H*-pyridin-1-yl)acetamido]-1(*N*′),2(*N*),2′(*N*′)-trimethyl-2,2′-diaminodiethylamine (L3). Some 10% Pd/C (0.07 g) was added to a solution of protected ligand **4** (0.70 g, 1.12 mmol) in dry MeOH (15 mL), and the mixture was hydrogenated (3 atm) for 12 h at room temperature. The catalyst was then filtered using a Celite pad, and the solution was concentrated. **L3** was obtained in quantitative yield (0.50 g) as a white solid: mp 119−122 °C dec; MS *m*/*z* (ESI) 470.3 ($[M + Na]^+$), 448.3 ($[M + 1]^+$); IR (film) 3450, 3382, 1655, 1581, 1272, 1238, cm^{-1}; ^{1}HNMR (D_2O) δ 6.95−6.62 (m, 4H), 6.33−6.10 (m, 2H), 4.83−4.77 (m, 4H), 3.56−3.37 (m, 4H), 3.05−2.98 (m, 4H), 2.88−2.60 (m, 6H), 2.41−2.27 (m, 3H); ^{13}CNMR (D_2O) δ 170.16, 169.65, 160.47, 160.29, 160.18, 147.76, 147.47, 147.11, 130.59, 120.14, 119.82, 109.63, 109.50, 109.31, 54.94, 54.48, 53.31, 52.65, 52.50, 51.95, 47.81, 46.00, 45.75, 43.55, 42.44, 35.88, 35.34, 35.05.

$[Cu(H_{-1}L2)]_2(ClO_4)_2 \cdot 3H_2O$ (5). A sample of $Cu(ClO_4)_2 \cdot 6H_2O$ (37 mg, 0.1 mmol) in water (30 mL) was added to an aqueous solution (30 mL) containing **L2**·$2HClO_4$ (64 mg, 0.1 mmol). The pH of the resulting solution was adjusted to 5.5 with 0.1 M NMe_4-OH; after a few minutes, **5** precipitated as a microcrystalline green solid (62 mg, 93%). Anal. Calcd for $C_{48}H_{72}Cl_2Cu_2N_{12}O_{23}$: C 41.68; H 5.25; N 12.15. Found: C 41.9; H 5.4; N 12.2. Crystal suitable for X-ray analysis was obtained by slow evaporation of a water solution containing **5**.

$[Cu(H_{-1}L3)](ClO_4) \cdot 3H_2O \cdot 0.5CH_3OH$ (6). 6 was obtained from **L3**·$HClO_4$ (58 mg, 0.1 mmol) and $Cu(ClO_4)_2 \cdot 6H_2O$ (37 mg, 0.1 mmol) by following the same procedure reported for **5**, giving a solid as green microcrystals (61 mg, 89%). Anal. Calcd for $[Cu(H_{-1}L3)](ClO_4) \cdot 3H_2O$, $C_{21}H_{36}ClCuN_5O_{14}$: C, 37.01; H, 5.32; N, 10.28. Found: C, 37.2; H, 5.4; N, 10.2. **6**, as green crystals suitable for X-ray analysis, was obtained by slow evaporation of the solvent of an aqueous diluted solution containing several drops of methanol.

$[Zn_2H_{-2}L1](ClO_4)_2 \cdot 4H_2O$. A sample of $Zn(ClO_4)_2 \cdot 6H_2O$ (37 mg, 0.1 mmol) in water (15 mL) was added to an aqueous solution (15 mL) containing **L1**·$2HClO_4$ (68 mg, 0.1 mmol). The pH of the resulting solution was adjusted to 7 with 0.1 M NMe_4OH; after 12 h the complex precipitated as a colorless microcrystalline solid (53 mg, 61%). Anal. Calcd for $C_{24}H_{44}N_6O_8Zn_2$: C, 32.97; H, 5.07; N, 9.61. Found: C, 32.8; H, 5.1; N, 9.5. MS (ESI) (*m*/*z*): 702−704 ($([Zn_2H_{-2}\mathbf{L1}]ClO_4)^+$), 301.5 ($([Zn_2H_{-2}\mathbf{L1}]ClO_4)^{2+}$). ^{1}H NMR ($D_2O$, pH = 7, 25 °C): δ 7.41 (d, 1H), 7.35 (d, 1H), 7.23 (d, 1H), 7.01 (d, 1H), 6.68 (dd, 1H), 6.58 (dd, 1H), 4.53 (t, 2H), 4.32 (t, 2H), 3.52 (t, 1H), 3.41 (t, 2H), 3.17 (m, 13H), 2.95 (m, 7H), 2.62 (s, 3H) ppm. ^{13}C NMR (chemical shift reported separately for the two conformers present in solution on the NMR time scale; see Spectroscopy): conformer **a**, 163.9, 156.1, 123.4, 116.3, 113.7, 60.1, 59.7, 54.6, 45.8, 40.9 ppm; conformer **b**, 161.8, 161.6, 118.5, 113.8, 110.6, 60.3, 59.9, 55.1, 54.2, 46.4, 46.2, 41.7, 41.4 ppm.

Caution. *Perchlorate salts of organic compounds are potentially explosive; these compounds must be prepared and handled with great care!*

X-ray Crystallography. For both compounds $[Cu(H_{-1}\mathbf{L2})]_2(ClO_4)_2 \cdot 3H_2O$ (**5**) and $[Cu(H_{-1}\mathbf{L3})](ClO_4) \cdot 3H_2O \cdot 0.5CH_3OH$ (**6**) intensity data collections were performed using a Siemens SMART diffractometer equipped with a CCD area detector and a rotating

anode. The SMART[20] software was used, and the radiation was Cu Kα ($\lambda = 1.5418$ Å). Five settings of ω were used, and narrow data "frames" were collected for 0.3° increments in ω. A total of 3000 frames of data were collected providing a sphere of data. Data reductions were performed with the SAINT 4.0[21] program. Absorption corrections were performed with the SADABS[22] program. Structures were then solved using the SIR97 program[23] and refined by full-matrix least squares against F^2 using all data (SHELX97).[24]

The independent complex **a** of compound **5** (see Results and Discussion) is affected by disorder: the carbon atoms bound to N(5), labeled as C(14), C(15), and C(16), have been split into two positions A and B with population parameters of 0.6 and 0.4, respectively. The two models show the methyl carbon atom C(15) pointing in two opposite directions: inside (model B) and outside (model A) the cavity is formed by the mean planes of the nitrogen atoms and the pyridinone moieties.

Due to the disorder, the hydrogen atoms bound to C(14), C(15), and C(16), as well as those of the carbon atoms C(13) and C(17), were not include in the refinement.

Concerning the acidic hydrogen atoms of the two ligands $[H_{-1}\mathbf{L2}]^-$ and $[H_{-1}\mathbf{L3}]^-$, **5** and **6**, respectively, only the one bound to N(5)′ (complex **b** of compound **5**) was introduced in the refinement as it was found in the Fourier difference map and refined isotropically. On the contrary all the hydrogen atoms bound to the carbon atoms of the ligands were introduced in calculated positions with temperature factors related to the atoms to which they are bound.

Finally, the perchlorate counterion of **5** is affected by a certain degree of disorder and the methanol molecule of **6**. In fact the perchlorate oxygen atom O(15) was found in two different positions and a population parameter of 0.5 was assigned to each one. The methanol molecule in **6** was quite close to an inversion center, and a population parameter of 0.5 was assigned to the carbon atom C(22) and to the oxygen atom O(14), while the hydrogen atoms of the methanol molecule were not introduced.

Anisotropic thermal parameters were used for the non H-atoms.

Geometrical calculations were performed by PARST97,[25] and molecular plots were produced by the program ORTEP3.[26]

Crystallographic data and refinement parameters are reported in Table 1.

EMF Measurements. Equilibrium constants for protonation and complexation reactions with **L1**−**L3** were determined by pH-metric measurements ($pH = -\log [H^+]$) in 0.15 M NMe_4Cl at 298.1 ± 0.1 K, using the fully automatic equipment that has already been described; the EMF data were acquired with the PASAT computer program.[27] The combined glass electrode was calibrated as a hydrogen concentration probe by titrating known amounts of HCl with CO_2-free NMe_4OH solutions and determining the equivalent point by Gran's method,[28] which gives the standard potential $E°$ and the ionic product of water ($pK_w = 13.83(1)$ at 298.1 K in 0.15 M NMe_4Cl, $K_w = [H^+][OH^-]$). At least three potentiometric titrations were performed for each system in the pH range 2−11, using different molar ratios of M/**L** ranging from 1:1 to 3:1. All titrations were treated either as single sets or as separate entities, for each system; no significant variations were found in the values of the determined constants. The HYPERQUAD computer program was used to process the potentiometric data.[29]

Table 1. Crystal Data and Structure Refinement Parameters for **5a,b** and **6**

param	**5a,b**	**6**
empirical formula	$C_{48}H_{72}Cl_2Cu_2N_{12}O_{23}$	$C_{21.5}H_{36}ClCuN_5O_{13.5}$
fw	1383.16	679.54
temp (K)	298	298
wavelength (Å)	1.5418	1.5418
crysl system, space group	triclinic, $P\bar{1}$	monoclinic, $P2_1/n$
a (Å)	9.127(1)	9.039(1)
b (Å)	13.840(1)	23.253(3)
c (Å)	24.104(2)	14.279(2)
α (deg)	83.810(2)	90
β (deg)	79.557(2)	96.339(7)
γ (deg)	88.682(2)	90
V (Å^3)	2976.9(5)	2982.9(7)
Z, calcd density (g/cm^3)	2, 1.543	4, 1.513
abs coeff (mm^{-1})	2.476	2.499
reflcns collcd/unique	13 284/7040	13 480/3905
data/params	6456/824	3433/388
goodness-of-fit on F^2	1.062	1.051
final R indices [$I > 2\sigma(I)$]	R1 = 0.0665, wR2 = 0.1913	R1 = 0.0710, wR2 = 0.2121
R indices (all data)	R1 = 0.0702, wR2 = 0.1950	R1 = 0.0761, wR2 = 0.2166

NMR Experiments. ^1H and ^{13}C NMR spectra were recorded on a Bruker Avance 200 instrument, operating at 200.13 and 50.33 MHz, respectively, and equipped with a variable-temperature controller. The temperature of the NMR probe was calibrated using the 1,2-ethandiol as calibration sample. For the spectra recorded in D_2O, the peak positions are reported with respect to HOD (4.75 ppm) for ^1H NMR spectra, while dioxane was used as reference standard in ^{13}C NMR spectra ($\delta = 67.4$ ppm). For the spectra recorded in $CDCl_3$ and DMSO-d_6 the peak positions are reported with respect to TMS. $^1H-^1H$ and $^1H-^{13}C$ correlation experiments were performed to assign the signals.

Results and Discussion

Synthesis. Scheme 1 outlines the preparation of the new multidentate ligand **L3**. The synthesis, similar to that reported for **L1**,[16] is based on the activation of the carboxylic function in **1** as *p*-nitrophenyl ester **2** followed by reaction with *N*,*N*′-dimethyl-*N*-(2-(methylamino)ethyl)ethane-1,2-diamine (**3**) affording the bis(amide) **4** in 65% yield. **L3** was obtained in almost quantitative yield from **4** by hydrogenolysis in a presence of 10% Pd/C.

The 3-(benzyloxy)-1-(carboxymethyl)-2(1*H*)-pyridinone (**1**) was prepared from the commercially available 2,3-dihydroxypyridine by following the procedure reported in ref 16. **1** was activated as *p*-nitrophenyl ester **2** with *p*-nitrophenol in DMF using 1,3-dicyclohexylcarbodiimide (DCC) as coupling agent. The activated ester was reacted with **3** in dry DMF in the presence of Et_3N. The product was purified by chromatography to obtain the bis-acylated product **4** in 65% yield. Subsequent removal of the protecting

(20) *SMART: Area-Detector Integration Software*; Siemens Industrial Automation, Inc.: Madison, WI, 1995.
(21) *SAINT*, version 4.0; Siemens Industrial Automation, Inc.: Madison, WI, 1995.
(22) Sheldrick, G. M. *SADABS*; University of Göttingen: Göttingen, Germany, 1996.
(23) Altomare, A.; Cascarano, G. L.; Giacovazzo, C.; Guagliardi, A.; Burla, M. C.; Polidori, G.; Camalli, M. *J. Appl. Crystallogr.* **1999**, *32*, 115.
(24) Sheldrick, G. M. *SHELX 97*; University of Göttingen: Göttingen, Germany, 1997.
(25) Nardelli, M. *Comput. Chem.* **1983**, *7*, 95.
(26) Farrugia, L. J. *J. Appl. Crystallogr.* **1997**, *30*, 565.
(27) Fontanelli, M.; Micheloni, M. *1st Spanish-Italian Congress for the Thermodynamics of Metal Complexes*; Peñiscola, Spain, June 3−6, 1990; University of Valencia: Valencia, Spain, 1990; p 41.
(28) (a) Gran, G. *Analyst* **1952**, *77*, 661. (b) Rossotti, F. J.; Rossotti, H. *J. Chem. Educ.* **1965**, *42*, 375.
(29) Gans, P.; Sabatini, A.; Vacca, A. *Talanta* **1996**, *43*, 1739.

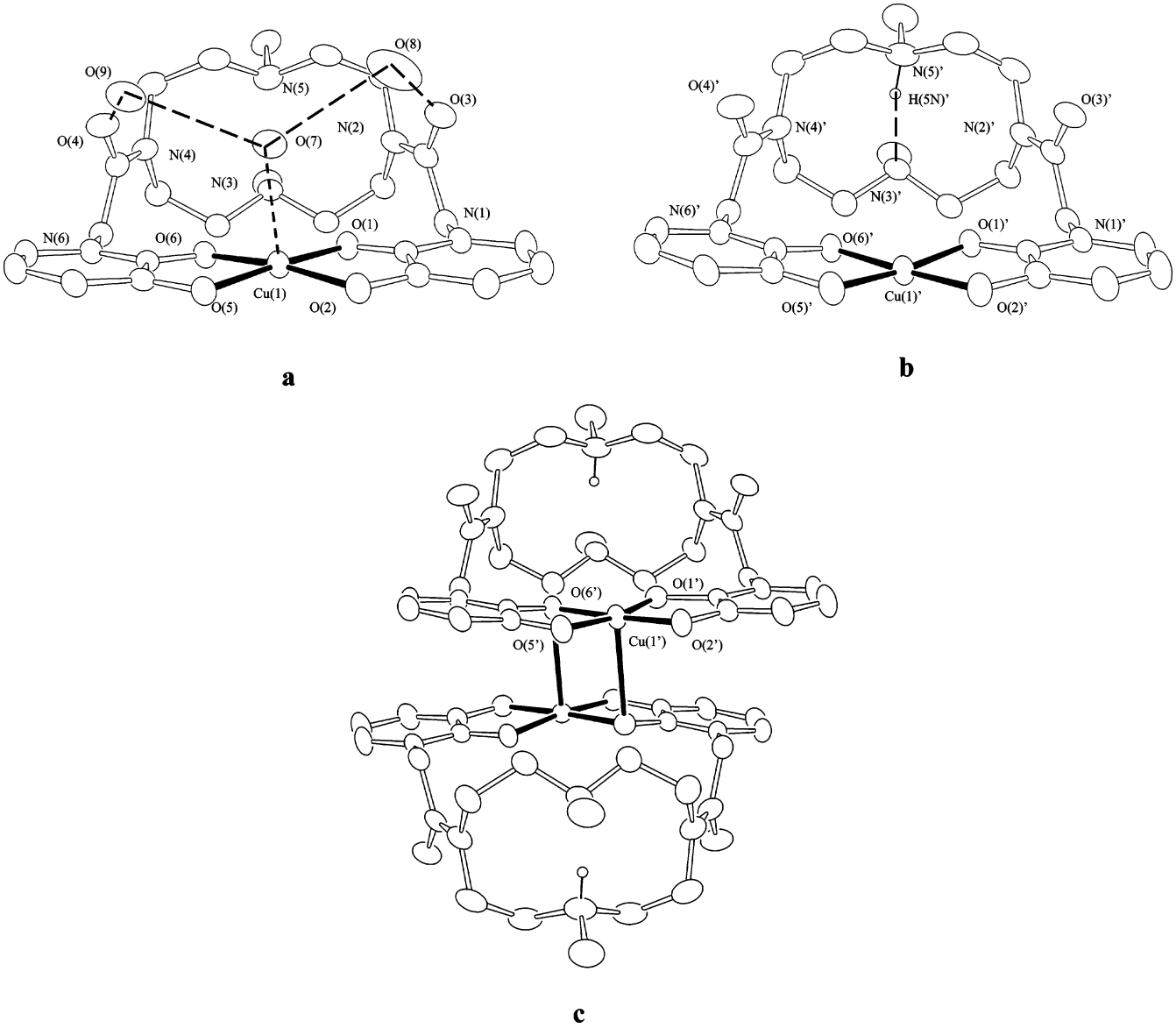

Figure 2. ORTEP view of the two independent complexes **a** (a) and **b** (b) of **5** and of the dimeric complex of **5** (c). Ellipsoids are drawn at 30% probability.

benzyl group by catalytic hydrogenolysis was achieved under pressure (3 atm) in MeOH, in the presence of 10% Pd/C, affording **L3** in quantitative yield.

Description of the Structures. $[Cu(H_{-1}L2)]_2(ClO_4)_2\cdot 3H_2O$ (5). The asymmetric unit contains two independent metal complexes (**a** and **b**, Figure 2). Both the copper atoms show a 4 + 1 square pyramidal (sp) coordination even though the environment is different because of the different nature of the donor in the fifth position. A water molecule is located at the apex of the sp in **a** (Cu(1)−O(7) = 2.425(4) Å), while in **b** the fifth coordination site is occupied by a pyridinone oxygen atom (Cu(1′)−O(6″) = 2.878(3) Å) provided by a symmetry related **b** complex (″ = $-x + 1, -y + 2, -z + 2$). In both complexes the copper ion is shifted toward the apical donor (0.1041(7) and 0.0767(7) Å in **a** and **b**, respectively). The angle formed by the Cu−O apical bond and the mean plane defined by the O(1)−O(6) [O(1′)−O(6′)] donor atoms is 87.6(1) and 77.65(8)° in **a** and **b**, respectively. In both the metal complexes, the $Cu\cdots O_{pyridinone}$ distances defining the base of the sp (Table 2) well compare with those found for Cu(II) complexes having analogous coordination spheres retrieved in the Cambridge Structural Database (CSD), V. 5.25,[30] while the bond distance involving the fifth donor is a little bit longer than those observed in related species.

The overall shapes of the two independent complex cations are very similar, as shown by the quite similar angles between the mean planes described by the nitrogen atoms of the cyclic amine moiety and the oxygen atoms coordinating the metal ion (75.7(2) and 78.7(2)° in **a** and **b**, respectively). Moreover, the superimposition of the $H_{-1}L2^-$ anion of the two independent complexes gives a root mean square value of 0.073. [Rms was calculated using all the non-hydrogen atoms, with the exception of the C(13)−C(14)−N(5)C(15)−C(16)−C(17) moiety that in **a** is affected by disorder; see Experimental Section.]

(30) Allen, F. H.; Kennard, O. Cambridge Structural Database. *J. Chem. Soc., Perkin Trans. 2* **1989**, 1131.

Table 2. Selected Bond Lengths (Å) and Angles (deg) for Complexes **a** and **b** of **5** and of **6**[a]

5a		**5b**		**6**	
Cu(1)−O(1)	1.960(3)	Cu(1′)−O(1′)	1.940(3)	Cu(1)−O(1)	1.944(3)
Cu(1)−O(2)	1.943(3)	Cu(1′)−O(2′)	1.922(3)	Cu(1)−O(2)	1.924(4)
Cu(1)−O(5)	1.935(3)	Cu(1′)−O(5′)	1.910(3)	Cu(1)−O(5)	1.921(4)
Cu(1)−O(6)	1.975(3)	Cu(1′)−O(6′)	1.962(3)	Cu(1)−O(6)	1.943(4)
Cu(1)−O(7)	2.425(4)	Cu(1′)−O(6″)	2.878(3)	Cu(1)−O(7)	2.568(8)
O(1)−Cu(1)−O(2)	85.6(1)	O(1′)−Cu(2)−O(2′)	86.2(1)	O(1)−Cu(1)−O(2)	85.2(2)
O(1)−Cu(1)−O(5)	175.7(1)	O(1′)−Cu(2)−O(5′)	173.5(2)	O(1)−Cu(1)−O(5)	174.8(2)
O(1)−Cu(1)−O(6)	93.5(1)	O(1′)−Cu(2)−O(6′)	93.5(1)	O(1)−Cu(1)−O(6)	89.3(2)
O(1)−Cu(1)−O(7)	94.4(1)	O(1′)−Cu(1′)−O(6″)	83.4(1)	O(1)−Cu(1)−O(7)	92.2(2)
O(2)−Cu(1)−O(5)	95.3(1)	O(2′)−Cu(2)−O(5′)	94.1(2)	O(2)−Cu(1)−O(5)	99.9(2)
O(2)−Cu(1)−O(6)	171.9(1)	O(2′)−Cu(2)−O(6′)	177.5(2)	O(2)−Cu(1)−O(6)	171.3(2)
O(2)−Cu(1)−O(7)	94.9(1)	O(2′)−Cu(1′)−O(6″)	98.1(1)	O(2)−Cu(1)−O(7)	106.5(2)
O(5)−Cu(1)−O(6)	85.0(1)	O(5′)−Cu(2)−O(6′)	85.9(1)	O(5)−Cu(1)−O(6)	85.8(2)
O(5)−Cu(1)−O(7)	89.7(1)	O(5′)−Cu(1′)−O(6″)	103.0(1)	O(5)−Cu(1)−O(7)	85.3(2)
O(6)−Cu(1)−O(7)	93.2(1)	O(6′)−Cu(1′)−O(6″)	84.3(1)	O(6)−Cu(1)−O(7)	80.5(2)

[a] ″ = $-x + 1, -y + 2, -z + 2$.

The [2424]C corner[31] conformation of the [12]aneN$_4$ ring of both the complexes, which can be ascribed to the sp^2 character of the nitrogen atoms[32] N(2) and N(4) in **a** [N(2′) and N(4′) in **b**] due to the usual amide π conjugation, allows N(3) [N(3′)] and N(5) [N(5′)] to approach each other (2.701(7) and 2.795(6) Å in **a** and **b**, respectively) with respect to the nitrogen atoms of the amide groups (5.421(6) and 5.429(7) Å in **a** and **b**, respectively). It is noteworthy that the Fourier map shows an electron density peak which has been ascribed to the acidic proton of the H$_{-1}$**L2**$^-$ of the **b** species bound to N(5′) and involved in a N−H···N short interaction with the facing nitrogen atom N(3′), the N···H distance being 1.95(9) Å. On the contrary, the disorder affecting the macrocyclic ring of complex **a** does not allow localization of the corresponding acidic hydrogen.

Concerning the crystal lattice, the way in which the Cu(1′) cation fulfills the fifth coordination site incomplex **b** results in dimers related by an inversion center (Figure 2c). In addition the couple of complexes is held together also by stacking interactions between the pyridinone rings, as revealed by the distances between the centroids of the facing aromatic rings (4.071(9) Å) and the angle formed by the normal to the pyridinone plane and the centroid vector (34.7(2)°).[33]

In addition to the coordinating water molecule (O(7)), the space delimited by the two mean planes containing the donor oxygen atoms [O(1), O(2), O(5), and O(6)] and the nitrogen atoms of the amine moiety N(2)−N(5) of complex **a** hosts two further crystallization water molecules, namely O(8) and O(9). These three molecules are held in place by a good network of hydrogen bonds also involving both the carbonyl oxygen atoms O(3) and O(4). Particularly, the oxygen atom O(3) is 2.708(7) Å from O(8), which, in turn, interacts with the coordinating O(7) (2.857(9) Å). The latter binds O(9) at 2.867(6) Å, which finally interacts with the carbonyl oxygen O(4) (2.827(5) Å). As a final point **a** complexes are arranged in chains held together by a pair of water molecules, so that the pyridinone oxygen atoms O(2) and O(5) are H-bonded to O(9)‴ and O(7)‴, respectively (‴ = $-x + 1, -y + 1, -z + 1$, distances O(2)···O(9)‴ = 2.926(5) and O(5)···O(7)‴ = 2.724(5) Å).

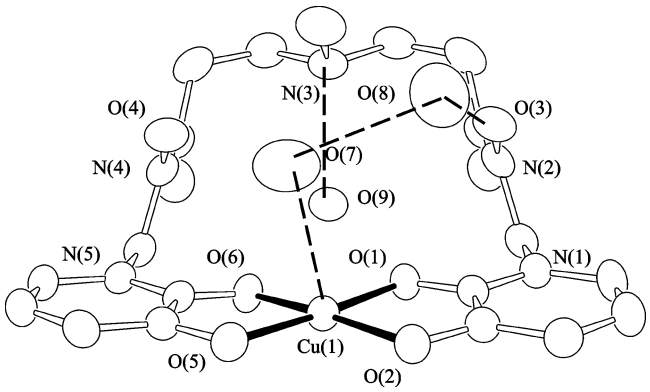

Figure 3. ORTEP view of the metal complex of **6**. Ellipsoids are drawn at 30% probability.

[Cu(H$_{-1}$L3)](ClO$_4$)·3H$_2$O·0.5CH$_3$OH (6). In the asymmetric unit there is one complex cation, a perchlorate anion, three water molecules, and a molecule of methanol with population factor of 0.5. The coordination environment of the metal ion (Figure 3) is very similar to that already shown by **a** in **5**, resulting in a 4 + 1 arrangement of the five donor atoms with the metal ion slightly displaced toward the apical donor (0.0427(7) Å). The Cu(1)−O(7) bond distance is a little bit longer than in **a** (2.568(8) vs 2.425(4) Å), with an angle between the Cu(1)−O(7) vector and the mean sp plane 76.6(2)°.

The overall shape of the ligand H$_{-1}$**L3**$^-$ is very similar to that already discussed for H$_{-1}$**L2**$^-$ in **5**, as revealed by the quite similar angles between the mean plane described by the three nitrogen atoms of the amine moiety and that defined by the oxygen atoms coordinating the metal ion (76.2(3)°). However, it can be observed that the methyl group bound to N(3) points inside the ligand cavity at variance with the corresponding −CH$_3$ group in **a** (model A with population factor 0.6) and **b**. As expected the amide nitrogen atoms N(2) and N(4) show the usual sp^2 geometry.

Also in this case the molecular cavity hosts two water molecules, in addition to the coordinating one (O(7)) all of

(31) *Stereochemical and Stereophysical Behaviour of Macrocycles*; Bernal, I., Ed.; Elsevier: Amsterdam, 1987; Vol. 2.
(32) Anelli, P. L.; Calabi, L.; Dapporto, P.; Murru, M.; Paleari, L.; Paoli, P.; Uggeri, F.; Verona, S.; Virtuani, M. *J. Chem. Soc., Perkin Trans. 1* **1995**, 2995.
(33) Janiak, C. *J. Chem. Soc., Dalton Trans.* **2000**, 3885.

Table 3. Protonation Constants (log *K*) of **L1**−**L3** Determined by Means of Potentiometric Measurements in 0.15 mol dm^{-3} NMe_4Cl Aqueous Solution at 298.1 K

	log *K*		
reacn	**L1**	**L2**	**L3**
$H_{-2}L^{2-} + H^+ = H_{-1}L^-$	>12[a]	10.79(1)[b]	9.23(1)[c]
$H_{-1}L^- + H^+ = L$	9.70(1)	9.08(1)	8.40(1)
$L + H^+ = HL^+$	8.39(1)	8.33(1)	6.87(1)
$HL^+ + H^+ = H_2L^{2+}$	7.74(1)	1.86(2)	
$H_2L^{2+} + H^+ = H_3L^{3+}$	2.30(3)		

[a] From ref 16. [b] From ref 17. [c] Values in parentheses are the standard deviations on the last significant figure.

which interact through a network of hydrogen bonds. The oxygen atom O(8) plays almost the same role in **6** and **a**; that is, it interacts with the carbonyl oxygen atom O(3) and with the water molecule labeled O(7) (bond distances 2.773(8) and 2.78(1) Å, respectively). In addition it is also in contact with an oxygen of the perchlorate anion (O(8)···O(10) = 2.87(1) Å). On the contrary, in **a** and **6**, molecules labeled O(9) occupy very different positions. However, a visual inspection of the two complexes showed that O(9) in **6** and N(3) in **a** are located very close each other. A comparison of the interatomic distances involving N(3) and N(2), N(4), and N(5) of the macrocyclic ring in **a** and those between O(9) and the three nitrogen atoms [N(2)−N(4)] of the amine moiety in **6** quantitatively supports this observation. In particular, O(9) is 2.683(6) Å from N(3) in **6** (the corresponding N(3)−N(5) distance is 2.701(7) Å in **a**), thus indicating a strong H-bond interaction which suggests that the acidic proton, not located in the Fourier map, is bound to N(3). The same molecule (O(9)) further interacts with the pyridinone oxygen atom O(6) (3.007(5) Å).

Finally, a comparison of the solid state conformation shown by the ligands H_{-1}**L2**$^-$ and H_{-1}**L3**$^-$, in compounds **5** and **6**, respectively and by the H**L2**$^+$ species[16] underlines that both the macrocyclic and the open chain ligands have a very similar overall shape. This observation confirms that the N−C═O moieties stiffen the whole molecular framework irrespective of the 12-membered ring or the dien open-chain.

However, several minor differences can be pointed out:

(1) The metal complexation (as in **a** and **b**) causes the pyridinone rings to stay closer than they are in the free ligand (H**L2**$^+$ species).

(2) The carbonyl groups of complex **6** point more inward compared to the ones in the other species.

(3) The methyl grouping bond to N(3) may point inside the ligand cavity (as in the complex cation **a** and in compound **6**) or outside (H**L2**$^+$ and complex cation **b**).

Solution Studies. Basicity of L3. Table 3 summarizes the basicity constants of **L3** as potentiometrically determined in 0.15 M NMe_4Cl aqueous solution at 298.1 K; the basicity constants of **L1** and **L2** are also reported in the table for comparison. The neutral compound **L3** behaves as a monoprotic base and as a diprotic acid under the experimental conditions used. As shown in Table 3, it can be present in solution as anionic species H_{-2}**L3**$^{2-}$, indicating the removal of the acidic hydrogen atom of each pyridinone moiety; moreover, it can add one proton to form the H**L3**$^+$ species.

Table 4. Logarithms of the Equilibrium Constants Determined in 0.15 mol dm^{-3} NMe_4Cl at 298.1 K for the Complexation Reactions of **L1**−**L3** with Cu(II) Ions

	log *K*		
reacn	**L1**	**L2**	**L3**
$M^{2+} + H_{-2}L^{2-} = MH_{-2}L$		16.32(1)[a]	13.63(2)
$M^{2+} + H_{-1}L^- = MH_{-2}L + H^+$	4.67(2)	5.83(1)	4.4(1)
$M^{2+} + H_{-1}L^- = MH_{-1}L^+$	13.24(3)	15.48(1)	11.94(1)
$M^{2+} + L = ML^{2+}$	11.44(3)		6.45(3)
$M^{2+} + HL^+ = MHL^{3+}$	7.72(3)		
$M^{2+} + H_2L^{2+} = MH_2L^{4+}$	3.95(4)		
$M^{2+} + MH_{-2}L = M_2H_{-2}L^{2+}$	12.47(4)		
$M_2H_{-2}L^{2+} + OH^- = M_2H_{-2}LOH^+$	2.5(3)		

[a] Values in parentheses are the standard deviations on the last significant figure.

By analysis of the protonation constants starting from the anionic species, it was found that **L3** shows quite similar protonation constant values for the three protonation steps ranging from 9.23 for log K_1 to 6.87 for log K_3. These values are in agreement with the topology of the ligands, indicating an easy availability of protonation sites. Moreover, while the value of the log K_1 is similar to that found for trimethylamine,[34] log K_2 and log K_3 are more similar to those of the HPO group, thus suggesting an involvement of the amine functions in the first protonation steps and of the deprotonated HPO groups in the subsequent steps. This hypothesis was also confirmed by UV−vis and fluorescence emission experiments, because the spectra and trend were similar to those previously reported for compounds **L1** and **L2**.[16,17] In a comparison of these values with those found for **L1** and **L2**, **L3** was shown to have lower basicity constants in each protonation step with respect to the other ligands; this aspect can be ascribed to the presence of only one amine group but also to the lack of the macrocyclic base in **L3** that leads to a lower preorganization of the ligand and thus of the HPO groups to stabilize the acidic protons by a hydrogen bond network.

Coordination of Cu(II) and Zn(II) Ions. The coordination properties of **L1**−**L3** were studied in 0.15 mol dm^{-3} NMe_4Cl aqueous solution at 298.1 K. The stability constants for the equilibrium reactions of the ligands with Cu(II) and Zn(II) were potentiometrically determined and are reported in Tables 4 and 5 for Cu(II) and Zn(II), respectively. **L1** forms mono- and dinuclear M(II) species, while **L2** and **L3** form only mononuclear complexes with both metal ions examined. In the case of **L1**, the dinuclear species are largely prevalent in aqueous solution when the ligand−metal ratio is 1:2; when the **L1**/M(II) molar ratio is 1:1, the mono- and dinuclear species coexist in solution. The distribution diagrams of the species for the system **L1**/M(II) in 1:1 and 1:2 molar ratios as a function of pH are depicted in Figure 4, while those of **L2**/M(II) and **L3**/M(II) systems are reported in Figure 5.

Mononuclear Complexes. All of the ligands form stable mononuclear complexes with both of the metal ions examined. In a comparison of the species having the same

(34) Amorim, M.; Ascenso, J.; et al. *J. Chem. Soc., Dalton Trans.* **1990**, 3449.

Table 5. Logarithms of the Equilibrium Constants Determined in 0.15 mol dm^{-3} NMe_4Cl at 298.1 K for the Complexation Reactions of **L1**−**L3** with Zn(II) Ions

	log *K*		
reacn	**L1**	**L2**	**L3**
$M^{2+} + H_{-2}L^{2-} = MH_{-2}L$		11.67(1)[a]	8. 87(2)
$M^{2+} + H_{-1}L^{-} = MH_{-2}L + H^{+}$	1.38(2)	0.88(2)	−0.36(3)
$M^{2+} + H_{-1}L^{-} = MH_{-1}L^{+}$	10.52(3)	11.12(2)	7.50(3)
$M^{2+} + L = ML^{2+}$	7.82(2)	6.10(2)	4.08(6)
$M^{2+} + HL^{+} = MHL^{3+}$	5.63(3)		
$MH_{-2}L + OH^{-} = MH_{-2}LOH^{-}$	3.74(3)	1.95	2.59
$M^{2+} + MH{-}_{2}L = M_2H_{-2}L^{2+}$	8.24(2)		
$M_2H_{-2}L^{2+} + OH_{-} = M_2H_{-2}LOH^{+}$	5.22(3)		

[a] Values in parentheses are the standard deviations on the last significant figure.

stoichiometry, the Cu(II) complexes show higher stability than those of Zn(II) with all three ligands. In the absence of the metal ion, the fully deprotonated species of **L1**, i.e., H_{-2}**L1**$^{2-}$, was not achieved although it is formed in a presence of the metal. This aspect does not permit the direct comparison of the stability constants for the addition of M(II) to the fully deprotonated $H_{-2}L^{2-}$ species of all ligands, while this is possible for the $H_{-1}L^{-}$ species. Among the three ligands, **L2** shows the highest value of the stability constant for the formation of $[MH_{-1}L]^{+}$ species while **L3** shows the lowest. For example, the values of the stability constants for the complexation reactions $M^{2+} + H_{-1}L^{-} = MH_{-1}L^{+}$ with Cu(II) are 15.48, 13.24, and 11.94 logarithmic units for **L2**, **L1**, and **L3**, respectively. These values, in the case of **L2** and **L3**, are similar to those for the addition of M(II) to the $H_{-2}L^{2-}$ species. This means that both the $H_{-2}L^{2-}$ and $H_{-1}L^{-}$ species show a similar tendency to add the metal for both ligands (see Table 4) and indicates that the addition of a proton to the $H_{-2}L^{2-}$ species does not involve the coordination groups. A similar behavior could be hypothesized also for **L1**. Furthermore, similar coordination environments can be suggested for the M(II) ions in both $[MH_{-1}L]^{+}$ and $[MH_{-2}L]$ species. In the case of **L2** and **L3**, the coordination area is probably formed by the two converging HPO sidearms which provide a coordination environment similar to that shown in the two crystal structures of the $[CuH_{-1}L]^{+}$ species of the two ligands here reported (Figures 2 and 3). In this way, the acidic proton in the $[MH_{-1}L]^{+}$ species results located on an amine function far from the coordination area also in solution. Comparing the values of the formation of the $[MH_{-1}L]^{+}$ species for the three ligands, we can observe that the value of the formation of this species with **L1** is intermediate with respect to those of **L2** and **L3** suggesting that although **L1** shows a higher number of coordination groups, it is less preorganized in binding one transition metal ion than **L2**.

Thus, a ranking for preorganization of the sidearms to bind one metal ion can be retrieved: the macrocyclic base preorganizes the HPO groups better than the open chain, but the best preorganization is obtained by linking the two sidearms to the macrocyclic base by a N−C═O amide group. The value of the constants relative to the addition reaction $M^{2+} + H_{-2}L^{2-} = MH_{-2}L$ (16.32 and 13.63 for M = Cu and 11.67 and 8.87 for M = Zn, for **L2** and **L3**, respectively) supports this trend. However, while the involvement of the amine functions in the coordination of one metal ion is excluded in the case of **L2** and **L3**, this is not possible for **L1** (see below).

L1 shows a higher number of mononuclear protonated species than **L2** and **L3** with both metal ions. This is due to the presence of more protonable sites in the $[MH_{-2}$**L1**$]$ species not all of which are involved in the coordination of the M(II) ions.

The Cu/L systems do not show hydroxylated species while the Zn/L systems show the formation of a $[ZnH_{-2}LOH]^{-}$ species for all ligands. The addition of the OH^{-} anion is similar in all cases. This aspect indicates an unavailability of the Cu(II) core to the secondary ligand in aqueous solution which instead is permitted for the Zn(II) species. In the hydroxylated species, a pentacoordination environment with a square pyramid geometry around the metal, as observed in the Cu(II) crystal structures, could be hypothesized at least for **L2** and **L3**, with a fifth coordination position occupied by the hydroxide anion.

Dinuclear Complexes. Only **L1** forms dinuclear complexes with the two metal ions. The $[MH_{-2}$**L1**$]$ species can coordinate another M(II) ion, giving the dinuclear species $[M_2H_{-2}$**L1**$]^{2+}$. The addition of the second cation is 12.47 and 8.24 logarithmic units for Cu(II) and Zn(II), respectively, indicating a favorable process. The considerably high values found for the addition of the second M(II) implies that the dinuclear species are largely prevalent in aqueous solution for a 2:1 M(II):**L1** molar ratio at pH values higher than 5 or 6.5 for Cu(II) and Zn(II), respectively (Figure 4b,d).

Unfortunately, in the absence of crystallographic data, it is difficult to suggest a coordination environment of the two metal ions, even though these values suggest that in the dinuclear species all parts of the molecular framework of the ligand, i.e., also the macrocyclic base, must be involved in the coordination of the two metal ions.

Both M(II)/**L1** systems show the formation of a hydroxylated dinuclear species. The constant values for the addition of the OH^{-} anion to the $[M_2H_{-2}$**L1**$]^{2+}$ complex are 2.5 and 5.22 logarithmic units for Cu(II) and Zn(II), respectively. The high value for the Zn(II) complex in comparison with the analogous constant for the addition of the OH^{-} anion to the corresponding mononuclear species (see Table 5) is indicative of a strong binding of the hydroxide ion in the $[Zn_2H_{-2}$**L1**$OH]^{+}$, leading us to suppose that this species is bound in a bridged arrangement between the two metal ions; this situation cannot be justified for the $[Cu_2H_{-2}$**L1**$OH]^{+}$ dinuclear species.

Spectroscopy. ^{1}H and ^{13}C NMR and UV−vis experiments in aqueous solution were performed to obtain further information about the coordination environment in the mono- and dinuclear complexed species.

^{1}H and ^{13}C NMR experiments were performed for the Zn(II)/**L2** system in D_2O solution; the ^{1}H NMR spectrum of the HPO resonances recorded at pH = 7.5, where the $[ZnH_{-1}$**L2**$]^{+}$ species is prevalent in solution (see Figure 5b), is reported in Figure 6 together with that of **L2** in the absence of Zn(II) recorded at the same pH value. The number and

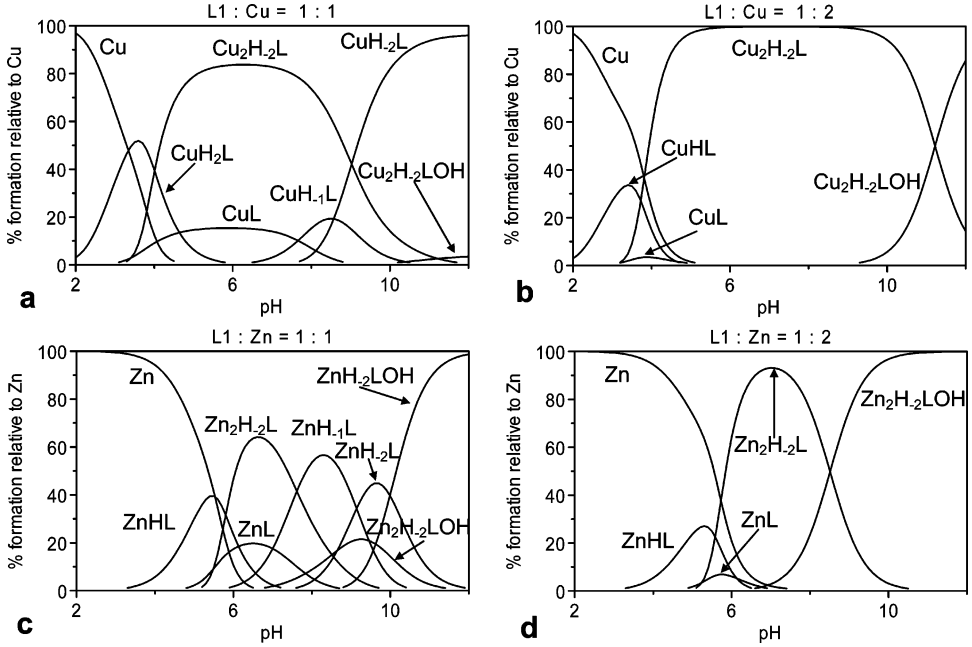

Figure 4. Distribution diagrams of the species for the **L1**/Cu(II) and **L1**/Zn(II) systems as a function of pH in aqueous solution. Conditions: $I = 0.15$ mol dm^{-3} NMe_4Cl at 298.1 K; [**L1**] $= 1 \times 10^{-3}$ mol dm^{-3}; (a) [Cu(II)] $= 1 \times 10^{-3}$ mol dm^{-3}; (b) [Cu(II)] $= 2 \times 10^{-3}$ mol dm^{-3}; (c) [Zn(II)] $= 1 \times 10^{-3}$ mol dm^{-3}; (d) [Zn(II)] $= 2 \times 10^{-3}$ mol dm^{-3}.

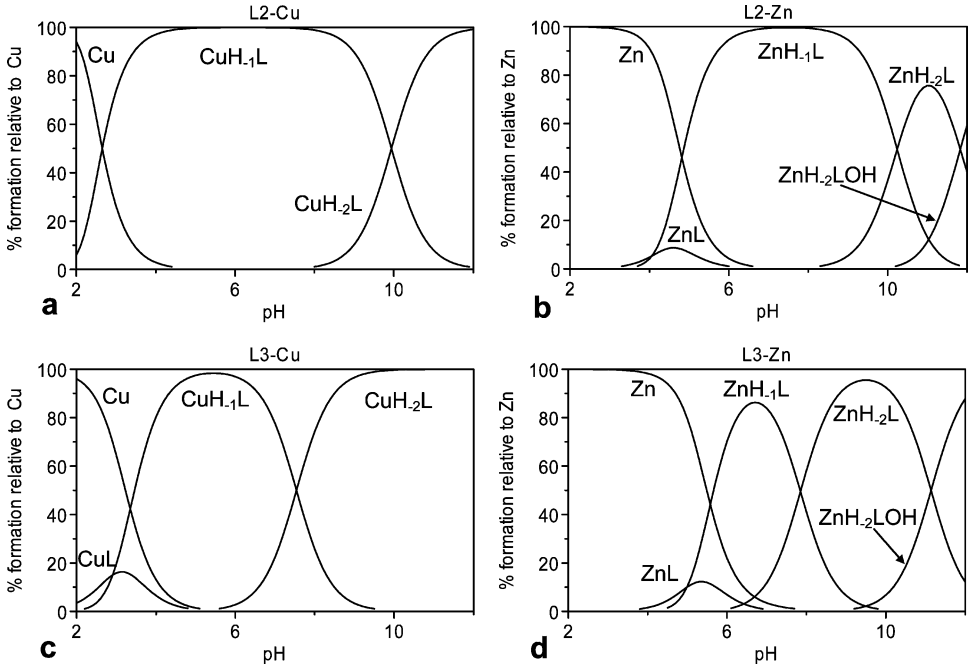

Figure 5. Distribution diagrams of the species for the L/M(II) systems as a function of pH in aqueous solution. Conditions: $I = 0.15$ mol dm^{-3} NMe_4Cl at 298.1 K; [L] = [M(II)] $= 1 \times 10^{-3}$ mol dm^{-3}; (a) **L2**/Cu(II) system; (b) **L2**/Zn(II) system; (c) **L3**/Cu(II) system; (d) **L3**/Zn(II) system.

form of the resonances in the spectrum of the $[ZnH_{-1}\mathbf{L2}]^+$ species highlight the fact that the two HPO sidearms are equivalent on the NMR time scale. These data are also supported by the ^{13}C NMR spectrum of this species, which shows only five resonances for the HPO carbon atoms. The resonance of the hydrogen atom H7 (in the *p*-position with respect to the carbonyl function) shows a downfield shift while those of the hydrogens H8 and H6 shift upfield with respect to those of the free ligand. The upfield shifts can be explained by the deprotonation of the HPO groups in the formation of the $[ZnH_{-1}\mathbf{L2}]^+$ species, while the downfield shift can be attributed to an involvement of the amide oxygen atom of each HPO group in the stabilization of the Zn(II) ion. The observed changes indicate that the coordination of Zn(II) mainly involves the HPO groups of **L2**; moreover, the symmetry showed by the sidearms suggests a coordination environment around the Zn(II) similar to that shown by Cu(II) in the crystal structure of the $[CuH_{-1}\mathbf{L2}]^+$ species. The analysis of the aliphatic resonances, as previously reported for the free ligand,[16] was complicated, due to the

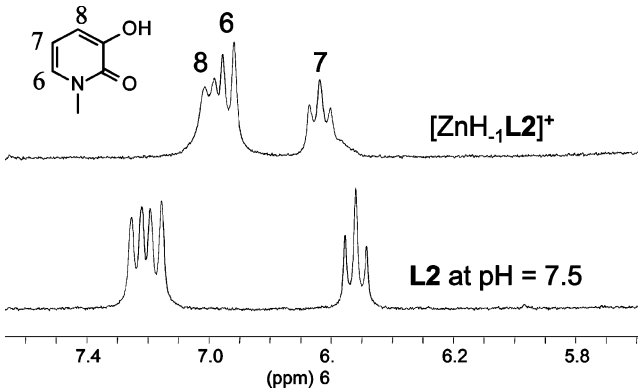

Figure 6. ^{1}H NMR spectra of the HPO resonances of the Zn/**L2** system of 1:1 molar ratio and **L2** recorded in aqueous solution at pH = 7.5.

presence of the amide functions in the macrocyclic base both in ^{1}H and ^{13}C NMR spectra, and thus they are not reported; however, they are quite similar in both systems supporting the hypothesis that the macrocyclic base is not directly involved in the coordination of the Zn(II) ion. This spectral feature of the HPO in chemical shifts and form of the signals was also preserved at higher pH values, suggesting a similar coordination arrangement also in the other complexed species.

Similar ^{1}H and ^{13}C NMR spectral behavior was observed in the case of **L3**/Zn system, supporting a similar coordination environment of the two HPO groups around the zinc ion also in this system and similar to that retrieved in the copper crystal structure (Figure 3).

The UV−vis spectra recorded in aqueous solution for the **L2** or **L3** systems containing Cu(II) or Zn(II) ions at different pH values support the previous hypothesis. For example, the spectrum recorded for system **L3**/Cu(II) at pH = 5.5, where the mononuclear species $[CuH_{-1}\mathbf{L3}]^+$ is prevalent in solution, shows two bands at λ_{max} 249 nm (ϵ = 11 900 cm^{-1} mol^{-1} dm^3) and 314 nm (ϵ = 19 200 cm^{-1} mol^{-1} dm^3) with a shoulder at 325 nm (ϵ = 14 200 cm^{-1} mol^{-1} dm^3) attributed to the n → π^* and π → π^* electronic transitions of HPO chromophores, respectively, a band at λ_{max} 384 nm (ϵ = 400 cm^{-1} mol^{-1} dm^3), and a large band at λ_{max} 717 nm (ϵ = 200 cm^{-1} mol^{-1} dm^3) due to the charge-transfer bands of the Cu(II) ion denoting a square planar geometry of the donor atoms around the metal. The spectral profile in solution of the $[Cu(H_{-1}\mathbf{L3})]^+$ species is equal to that recorded on the crystals of the $[Cu(H_{-1}\mathbf{L3})](ClO_4)\cdot 3H_2O\cdot 0.5CH_3OH$ species in the solid state, hinting that the coordination environment in the solid state (Figure 3) is preserved also in solution. This spectral profile is preserved in solution at higher pH values denoting that the coordination environment around the Cu(II) ion also remains unchanged in the $[CuH_{-2}\mathbf{L3}]$ species.

Similar spectral profiles were also observed in the case of Cu(II)/**L2** system supporting, also in this case, a coordination of the Cu(II) similar to that depicted in the crystal structure of the $[Cu(H_{-1}\mathbf{L2})]^+$ species, in aqueous solution too.

The Zn(II)/**L3** and Zn(II)/**L2** systems show spectral behavior similar to that of the Cu(II) systems in the UV region once again supporting a similar coordination environment of the two HPO around the Zn(II) ion in both systems.

Different spectral behavior was found in the case of the M(II)/**L1** systems. The UV spectrum of the Cu(II)/**L1** system in a 1:1 molar ratio, recorded at pH = 11 where the $[CuH_{-2}\mathbf{L1}]$ species is prevalent in solution, shows bands at λ_{max} 253 nm (ϵ = 12 400 cm^{-1} mol^{-1} dm^3) and 309 nm (ϵ = 19 600 cm^{-1} mol^{-1} dm^3) with a shoulder at 326 nm (ϵ = 13 900 cm^{-1} mol^{-1} dm^3) and a large band centered at λ_{max} 619 nm (ϵ = 400 cm^{-1} mol^{-1} dm^3). This spectrum is similar in the UV region to those observed for the Cu(II)/**L2** and **L3** system but quite different in the visible range. In this case, a blue-shift of the band at the lowest energy was observed while the band around 400 nm was missing. This suggests a different coordination environment of the Cu(II) ion in the $[CuH_{-2}\mathbf{L1}]$ species in aqueous solution with respect to the other mononuclear systems, although the involvement of at least an HPO group can be hypothesized. The spectral profile is preserved also in the dinuclear Cu(II)/**L1** species, but the band at 619 nm shows an absorptivity almost double that in the mononuclear one (ϵ = 750 cm^{-1} mol^{-1} dm^3) suggesting a coordination environment for both metal ions similar to that of the mononuclear species. The different coordination environment of Cu(II) in the complexed species with **L1** compared with those with **L2** or **L3** was also clearly seen by the blue color of the solution of the Cu(II)/**L1** systems with respect of the green color of the solution of the Cu(II)/**L2** or Cu(II)/**L3** systems.

The ^{1}H NMR spectrum of the system Zn(II)/**L1** in a 1:1 molar ratio recorded at pH = 11, where the $[ZnH_{-2}\mathbf{L1}OH]$ species is prevalent in solution, shows a broad profile, both in the aliphatic as well as in the aromatic part; moreover, the species is scarcely soluble preventing ^{13}C NMR experiments and thus not permitting reliable analysis. Instead, the ^{1}H and ^{13}C NMR spectra recorded on the Zn(II)/**L1** system in a 2:1 molar ratio gave sharp signals. The ^{1}H NMR spectrum of this system recorded at pH 7, where the $[Zn_2H_{-2}\mathbf{L1}]^{2+}$ species is prevalent in solution, is reported in Figure 7x. At a first glance, the HPO moieties show six resonances for the hydrogen atoms H6, H7, and H8, each integrating one proton. This could suggest that the two HPO groups behave independently in the complex; but after 12 h, a colorless amorphous solid (see Experimental Section) separates in the sample and the new spectrum, recorded on the filtered solution, highlights the decrease in three of the HPO resonances, as reported in Figure 7y. Similar behavior can be also observed in the field of the aliphatic resonances. This behavior can be justified by the presence of two different conformers of the complexed $[Zn_2H_{-2}\mathbf{L1}]^{2+}$ species which slowly interchange on the NMR time scale and not as previously hypothesized by two independently HPO groups in one $[Zn_2H_{-2}\mathbf{L1}]^{2+}$ species. In other words, two different conformations of the complex $[Zn_2H_{-2}\mathbf{L1}]^{2+}$ (called **a** and **b** in Figure 7) are present in solution in an approximately equimolar ratio at room temperature; one is more insoluble (species **b**) and precipitates first (it was impossible to detect if the precipitate also contains species **a**). This produces an impoverishment of species **b** in solution as

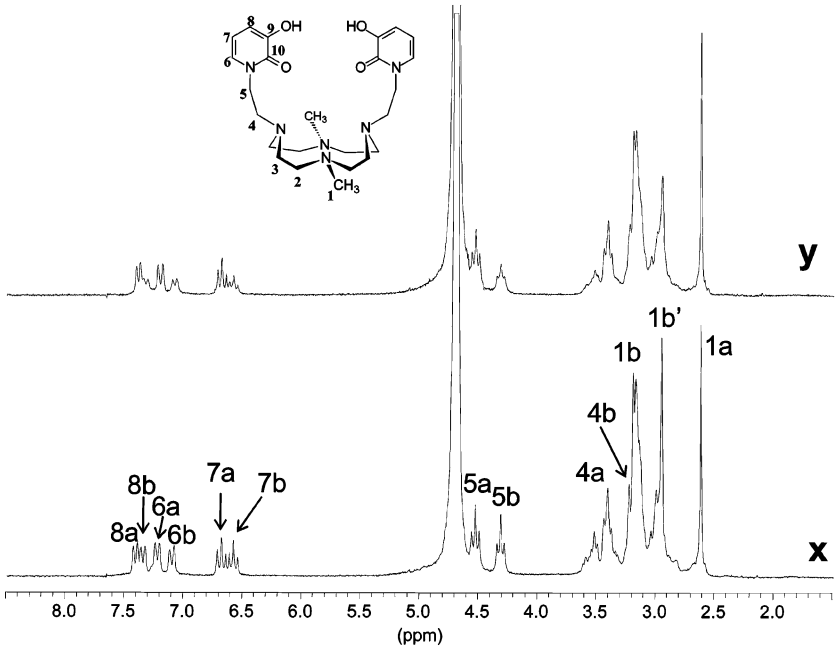

Figure 7. ^{1}H NMR spectra of the Zn/**L1** system of 2:1 molar ratio recorded in aqueous solution at pH = 7.0: spectrum recorded at time 0 (x); spectrum recorded after the precipitation of the solid (y).

shown by Figure 7y; the two species do not interchange fast at room temperature, and thus, the spectrum recorded after 12 h shows the prevalence of the species **a**. With warming of the solution of spectrum y and cooling it again at room temperature, the signals of the two conformers **a** and **b** in equimolar ratio, i.e. spectrum x, can be reobtained. At higher temperatures, the six resonances of the HPO observed at rt (room temperature) reveal a slow intermediate exchange on the NMR time scale, achieving a complete fast exchange (species **a** = species **b**) up to 350 K. After analysis of the spectrum in Figure 7x, the two HPO groups are equivalent in each $[Zn_2H_{-2}\mathbf{L1}]^{2+}$ conformers **a** and **b**, on the NMR time scale; this denotes a high symmetry of the two complexed species, at least for the HPO moieties. These data are confirmed by the ^{13}C NMR experiments that together with ^{1}H−^{1}H and ^{1}H−^{13}C correlation experiments permitted the assignment of the signal in the ^{1}H NMR spectrum of Figure 7x. The ^{13}C NMR spectrum recorded at pH 7 shows a total of 10 signals attributed to conformer **a** of which 5 are due to the HPO and 5 due to the aliphatic resonances; instead, the conformer **b** shows a total of 13 signals of which 5 are once again due to the HPO and 8 due to the aliphatic resonances. In other words, the conformer **a** shows a higher symmetry with respect to the conformer **b**; the different symmetry is retrieved in the macrocyclic base. This aspect is also underlined by the signals produced by the hydrogen atoms of the methyl groups in the ^{1}H NMR spectrum: complex **a** shows only one signal while **b** shows two signals for the two methyl groups of **L1** (1a, 1b, and 1b′ in Figure 7x). If one takes into account the topology of the ligand, as well as the previous studies performed on the possible conformation of **L1**, two possible conformers of the dinuclear $[Zn_2H_{-2}\mathbf{L1}]^{2+}$ species can be suggested and are reported in Figure 8. The two conformers of the $[Zn_2H_{-2}\mathbf{L1}]^{2+}$ species probably show the two main conformations of **L1** previously

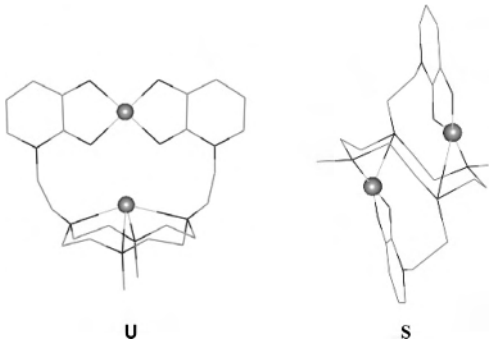

Figure 8. Proposed models for the U and S shape of the $[Zn_2H_{-2}\mathbf{L1}]^{2+}$ species.

called U- or S-shaped.[17] They are given by the relative position of the two HPO groups with respect to the macrocyclic base; they can stay on the same (U shape) or on the opposite part (S shape) with respect to the macrocyclic base. In the species with a U shape the two Zn(II) ions could be coordinated one by the four oxygen atoms of the two HPO moieties and the other one by the four amine functions of the macrocyclic base; in the other conformer (S shape), the two Zn(II) ions could be each coordinated by one HPO group and by some of the amine functions of the base as schematically reported in Figure 8. It is difficult to attribute one of the two conformers **a** or **b** to one of the two shapes. The signals of the spectra recorded at pH 10.5, where the $[Zn_2H_{-2}\mathbf{L1}OH]^{+}$ species is prevalent, became a little bit broad although they preserve similar chemical shifts of the previous one underlining the presence of the two conformers also in this species.

In a comparison of the information obtained by the NMR experiments on the Zn systems with those obtained by the UV−vis spectra on both Zn and Cu systems, the S shape seems to be the preferred conformer in the case of the Cu/

L1 system, since the band at 400 nm that the conformer with a U shape should show is absent in the UV spectra.

Conclusions

The new ligand **L3** was synthesized, and the coordination behavior toward the transition metal ions Cu(II) and Zn(II) of **L3** and those of the two analogous ligands **L1** and **L2** was investigated. All ligands show two HPO groups attached to a different polyaza fragment. Among the three ligands, only **L1** is able to form dinuclear species with both metal ions while **L2** and **L3** show only mononuclear species in aqueous solution.

When attention was focused on the preorganization of the two HPO groups, i.e., two binding sidearms, in binding one transition metal ion, the data obtained indicate that the macrocyclic base preorganizes the HPO groups better than the open chain but the best preorganization is obtained linking the two sidearms to the macrocyclic base by a N−C═O amide group as in **L2**.

In the case of **L2** and **L3**, the HPO groups bind the M(II) ion with all their oxygen atoms, giving rise to a tetracoordination environment of the two HPO in a square planar geometry around the M(II) ion in solution as well as in the solid state. The latter was evidenced by the two Cu(II) crystal structures with **L2** and **L3** here reported. In the structures, which had very similar overall shapes, the two HPO rings as well as the Cu(II) ion stay approximately on the same plane. The fifth position at the apex of square pyramidal geometry is occupied by a water molecule or a donor provided by a symmetry-related complex in the solid state; this position cannot be achieved by secondary ligands such as the hydroxide anion in solution. Instead, a fifth coordination position of Zn(II) can be replaced by adding an external species from the medium. In the case of the mononuclear species of Cu(II) with **L1** the UV−vis data seem to exclude this coordination environment.

Stable dinuclear complexes are allowed only for **L1**. Two conformations of the ligand around the metal ions have been suggested: a U and a S shape both of which are present in equimolar ratio in the Zn(II) dinuclear species while only the S shape seems to be present in the species with Cu(II).

The NMR experiments highlighted the presence of the two conformations which give rise to the coexistence in aqueous solution of two conformers of the dinuclear Zn(II)−**L1** species, slowly interchanging on the NMR time scale and having different solubility.

An external species can be bound by both dinuclear $[M_2H_{-2}\mathbf{L1}]^{2+}$ species, and in the case of the Zn(II), it can bridge the two Zn(II) ions. This aspect suggests a possible extension in the use of the mono- and dinuclear species as metal receptors for suitable external species in supramolecular and biomimicking chemistry.

Acknowledgment. We thank the Italian Ministero dell'Istruzione dell'Università e della Ricerca (MIUR), Grant PRIN2002, for financial support and the CRIST (Centro Interdipartimentale di Cristallografia Strutturale, University of Florence), where the X-ray measurements were carried out.

Supporting Information Available: Crystallographic data, positional parameters, isotropic and anisotropic thermal factors, and bond distances and angles in CIF format. This material is available free of charge via the Internet at http://pubs.acs.org.

IC0484607